Nuclear Science and Techniques (2025) 36:198
https://doi.org/10.1007/s41365-025-01751-y

New low-lying positive-parity states in ^{91}Ru: systematics of three-neutron-hole $\nu g_{9/2}^{-3}$ excitations in $N = 47$ even-odd isotones

Yong Zheng[1] · Meng Wang[1] · Min-Liang Liu[1] · Kai-Long Wang[1]

Received: 2 December 2024 / Revised: 4 February 2025 / Accepted: 12 February 2025 / Published online: 13 August 2025

Abstract
The low-energy excited states in the neutron-deficient nucleus ^{91}Ru were populated via the ^{58}Ni(^{36}Ar, $2p1n\gamma$)^{91}Ru reaction at a beam energy of 111 MeV. Charged particles, neutrons, and γ rays were emitted in the reactions and detected using a DIAMANT CsI ball, neutron wall, and EXOGAM Ge clover array, respectively. Angular-correlation and linear polarization measurements were performed to determine the spins and parities of the excited states unambiguously. In addition to the previously reported states, a new low-energy-level structure of ^{91}Ru, including one $7/2^+$ and two $11/2^+$ states, was established. Similar structures have also been reported in lighter $N = 47$ even-odd isotones down to ^{85}Sr, which were expected to come from the three-neutron–hole $\nu g_{9/2}^{-3}$ configuration. A semiempirical shell model was used to explain the level systematics of the $N = 47$ even-odd isotones. Calculated results indicated that the $7/2^+$ and the $11/2_1^+$ states are mainly associated with the seniority-three $\nu(g_{9/2})^{-3}$ excitations, while the $11/2_2^+$ level is most likely interpreted as a seniority $\upsilon = 1$ configuration of three neutron holes in the $\nu g_{9/2}$ orbital weakly coupled to a 2^+ excitation of the ^{88}Sr core. A comparison between the calculation and experiment shows that the two $11/2^+$ excited states display an increase in mixing with proton number Z added from ^{87}Zr up to ^{91}Ru.

Keywords Level structure · Three-neutron-hole excitation · Semiempirical shell model · Configuration mixing

1 Introduction

The existence of multi-quasiparticle configurations is consistently predicted in the low-energy-level structures of the nuclei near the $N = 50$ closed shell. For $N = 47$ even-odd nuclei, three-quasiparticle excitations are expected to dominate the level schemes, and the simplest excitations available will come from the three-neutron-hole $\nu g_{9/2}^{-3}$ configuration. Under the Pauli principle, the coupling of three $\nu g_{9/2}$ neutron holes generates spins from $J^\pi = 3/2^+$ to $21/2^+$ except for $19/2^+$. Indeed, the $7/2^+$ and $11/2^+$ states identified in the low-energy level schemes of the $N = 47$ even-odd isotones ^{85}Sr ($Z = 38$) [1–3], ^{87}Zr ($Z = 40$) [4, 5], and ^{89}Mo ($Z = 42$) [6–8] have been widely suggested to arise from the configuration of $\nu g_{9/2}^{-3}$.

By contrast, in the $N = 47$ isotones heavier than ^{85}Sr, the $\pi g_{9/2}$ protons become more active as the proton number Z increases and play an important role in building low-lying positive-parity levels. For example, a study on high-spin states in ^{89}Mo [6–8] proposed that strongly populated positive-parity states of up to $25/2^+$ are mainly built from the seniority-three $\pi g_{9/2}^2 \nu g_{9/2}^{-1}$ configuration. Therefore, it is of great interest and challenge to search for the low-lying $7/2^+$ and $11/2^+$ levels in ^{91}Ru ($Z = 44$), which will extend the systematic trend of the seniority-three $\nu g_{9/2}^{-3}$ configuration in the $N = 47$ nuclei to larger proton numbers and provide an ideal case for studying the competition between proton-particle and neutron-hole excitations from the $g_{9/2}$ orbitals.

The excited states in ^{91}Ru were investigated by Arnell et al. [9] via (α, xn) reactions. Subsequently, the level scheme was extended to J^π=$41/2^-$ at an excitation energy of 8 MeV by Heese et al. [10] using the reaction ^{58}Ni(^{36}Ar, $2p1n$)^{91}Ru at a beam energy of 149 MeV.

Fusion-evaporation reactions are crucial for populating excited states in nuclei and synthesizing superheavy nuclei [11–13]. This reaction mechanism results in a large

✉ Yong Zheng
zhengyong@impcas.ac.cn

[1] Institute of Modern Physics, Chinese Academy of Sciences, Lanzhou 730000, China

excitation energy and angular momentum in the nucleus. However, this reaction populates a considerable number of exit channels, complicating the selection of a specific channel for this study. As a typical solution, data analysis often involves using auxiliary measurements to detect charged particles and neutrons simultaneously [14]. In this paper, we report the results of a low-energy fusion-evaporation reaction designed to populate low- to medium-spin states in nuclei in the $A \sim 90$ mass region. The experiment and data analysis will be briefly described in the next section, followed by the details of the semiempirical shell model calculation we performed to interpret our data together with the level systematics along the $N = 47$ even-odd isotonic chain.

2 Experimental details and methods

The experiment was performed using the fusion-evaporation reactions ^{36}Ar + ^{58}Ni at a bombarding energy of $E(^{36}\mathrm{Ar}) = 111$ MeV. The beam was delivered using the GANIL CIME cyclotron and focused on a 99.83% isotopically enriched 6.0 mg/cm^2 thick ^{58}Ni target. The low-spin states in ^{91}Ru were populated in the $2p1n$ exit channel of the ^{36}Ar + ^{58}Ni fusion-evaporation reactions. Charged-particle emission following the decay of the ^{94}Pd compound nucleus was detected using a DIAMANT detector system consisting of 80 CsI scintillators [15, 16]. The Neutron Wall [17], comprising 50 liquid scintillator detectors covering a solid angle of 1π in the forward direction, was used to detect the evaporated neutrons. γ rays emitted from the reaction products were detected using an EXOGAM Ge clover detector array [18]. In the experiment, seven segmented clover detectors were placed in an angle of 90° and four detectors at an angle of 135° relative to the beam direction, leaving room for the Neutron Wall at forward angles. EXOGAM was used in a close-packed configuration, with the front part of the BGO Compton suppression shield removed from the clover detector (Further details can be found in Ref. [19]). Events were collected when at least one γ-ray was detected in the Ge clover detectors, coinciding with at least one neutron in the Neutron Wall. Under these conditions, 4×10^9 events were recorded.

In the offline analysis, the reaction channel leading to ^{91}Ru was selected by sorting events containing two protons fired in the DIAMANT CsI detectors together with one detected neutron. By using this filter, approximately 2.6×10^7 γ–γ coincidence events were selected. The event data were mainly from the $2p1n$ reaction channel, with some contamination from other channels, such as $3p$ and $3p1n$ which were the main reaction channels in this experiment. The efficiency and energy calibrations of the Ge clover detectors were performed using a standard radioactive γ-ray source ^{152}Eu. After the gain matching of all the Ge clover detectors, the coincidence data were sorted into symmetric and asymmetric (angle-dependent) matrices for subsequent analysis.

The spin and parity of the levels were deduced from information on both the directional correlations of the γ rays from the oriented states (DCO ratios) [20] and γ-ray polarization asymmetries [21]. In the γ-ray decay process, the emitted photon has an integer intrinsic spin L, which is called the multipolarity of γ radiation (for example, $L = 1, 2$ refer to dipole and quadrupole radiation, respectively). When a nucleus decays from an excited state, the angular momentum L carried by the γ transition is determined by the selection law $L \geqslant \Delta J = |J_\mathrm{i} - J_\mathrm{f}|$ where J_i and J_f are the spins of the initial and final nuclear states, respectively. In practice, only the two lowest multipolarities allowed by the selection law are observed; among them, the $L = \Delta J$ transition is called stretched radiation. The DCO ratio extracted directly in this experiment($R_\mathrm{DCO}^\mathrm{exp}$) has a value of ~1 for known pure stretched ($\Delta J = 2$) quadrupole transitions and of ~0.6 for known stretched ($\Delta J = 1$) dipole transitions when gating on quadrupole transitions. However, if the gate is set on a pure stretched dipole transition, the values will become ~1.6 and ~1, respectively. Normalization should be performed for the DCO ratio such that the effect of the gating transition type can be canceled. The normalized DCO ratio ($R_\mathrm{DCO}^\mathrm{norm}$) is defined as:

$$R_\mathrm{DCO}^\mathrm{norm} = a \cdot R_\mathrm{DCO}^\mathrm{exp}, \tag{1}$$

where a is a factor with a value of 1 when gating on the quadrupole transitions or 0.6 if the gate is set on the dipole transitions. The multipolarity of the emitted γ rays has been determined in this work based on the $R_\mathrm{DCO}^\mathrm{norm}$ value, which is ~ 1 for known pure stretched quadrupole transitions and is ~ 0.6 for known stretched dipole transitions.

The linear polarization of γ-ray transitions, which indicates their electromagnetic nature, is extracted from the scattering asymmetry between the planes perpendicular and parallel to the reaction plane. The measurement was facilitated using an EXOGAM clover detector with four crystals in one cryostat, wherein each crystal can operate as a scatterer and the adjacent crystals as absorbers. This asymmetry is represented as:

$$A = \frac{[bN_\perp] - N_\parallel}{[bN_\perp] + N_\parallel}, \tag{2}$$

where $N_\perp$ and $N_\parallel$ are the numbers of scattered photons of a given γ ray, which are scattered perpendicular and parallel to the reaction plane, respectively. These were extracted from their respective asymmetric matrices. Parameter b is the inherent geometrical asymmetry of the detection system and is estimated from the measure of asymmetry between the parallel and perpendicular scattering of γ-rays from an unpolarized radioactive source, for which, ideally, $N_\perp = N_\parallel$,

but is actually $bN_{\perp} = N_{\parallel}$. The value of b was obtained from measurements using a standard ^{152}Eu radioactive source of 1.05(3).

The polarization asymmetry A is negative for stretched purely magnetic transitions and positive for stretched purely electric transitions. Note that for mixed $M1 + E2$ transitions, the $R_{\mathrm{DCO}}^{\mathrm{norm}}$ ratios can vary between 0.6 and 1.0, depending on the δ multipole mixing ratio of the γ-ray. Further ambiguity arises for nonstretched ($\Delta I = 0$) pure $E1$ (or $M1$) transitions, where $R_{\mathrm{DCO}}^{\mathrm{norm}}$ for a nonstretched dipole transition with $\delta \approx 0$ mixing ratio is approximately the same as that for a stretched quadrupole transition [22, 23]. These ambiguities can be resolved by simultaneously measuring the linear polarizations of the γ-ray transitions. For example, stretched $E1$, $E2$ or unstretched $M1$ transitions and stretched $M1$ or unstretched $E1$ transitions have opposite linear polarization values [23]. Therefore, to determine the multipolarity and electromagnetic nature of a transition, both the DCO ratio and the polarization asymmetry should be measured.

3 Results

The partial-level scheme for ^{91}Ru shown in Fig. 1 was established based on an analysis of γ-ray coincidence relationships. Spin parity assignments were derived from an analysis of the normalized DCO ratios and Compton asymmetries.

Note that stretched quadrupole transitions cannot be distinguished from $\Delta I = 0$ dipole transitions or certain mixed $\Delta I = 1$ transitions based only on DCO ratios. In these cases, simultaneously measuring the linear polarizations of the transitions can provide supporting arguments for spin assignments. Figure 2 illustrates a two-dimensional plot of the asymmetries as a function of the normalized DCO ratios. As shown in the plot, the polarization and multipolarity measurements together provided reasonable spin parity assignments for the levels.

New transitions were assigned to ^{91}Ru based on coincidences with γ rays already known in this nucleus. Typical prompt γ-γ coincidence spectra for ^{91}Ru are shown in Fig. 3. The γ-ray transitions of ^{91}Ru are listed in Table 1. Their relative intensities were obtained from the total projection of the $E_\gamma - E_\gamma$ matrix. If the peak-to-background ratio in the total projection was too low or if there was contamination in the peak from other γ-ray transitions, the relevant transition energies were selected in the coincidence matrix, and the obtained projected spectra were used to fit the relative intensities. The transition energies were also measured from the total projection of the matrix. The energy uncertainties presented in the table are the sums of the statistical and calibration errors.

Below the previously known $13/2^-$ level at 1893 keV, a transition sequence consisting of 1003 keV and 890 keV

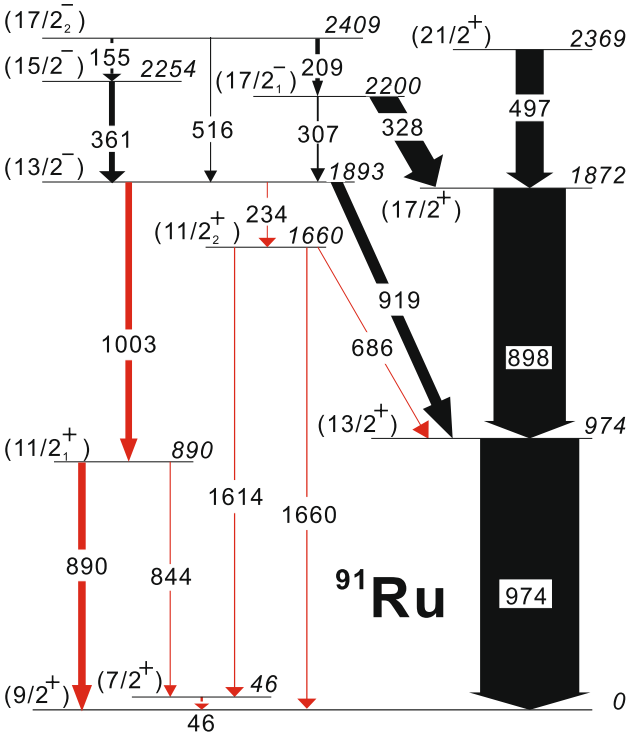

Fig. 1 (Color online) Partial low-energy level scheme of ^{91}Ru established by this work. The newly observed transitions are indicated by red arrows. The widths of the arrows represent the relative intensities of the γ rays

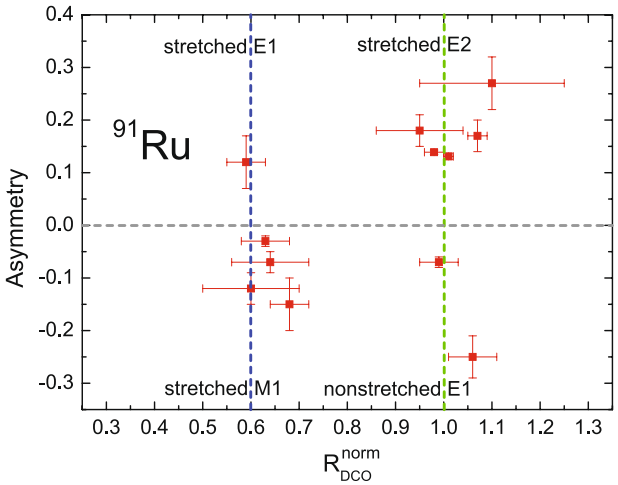

Fig. 2 (Color online) Two-dimensional plot of the asymmetries as a function of the normalized DCO ratios ($R_{\mathrm{DCO}}^{\mathrm{norm}}$s) of the γ rays shown in the partial decay scheme of ^{91}Ru (see Fig. 1). Stretched $E1$, $E2$, and $M1$ transitions and nonstretched $E1$ transitions are indicated in the plot. The dashed lines parallel to the y-axis correspond to the values obtained for known pure stretched dipole and quadrupole transitions, respectively. These lines have been drawn to guide the eye. For the definition of $R_{\mathrm{DCO}}^{\mathrm{norm}}$, see the text

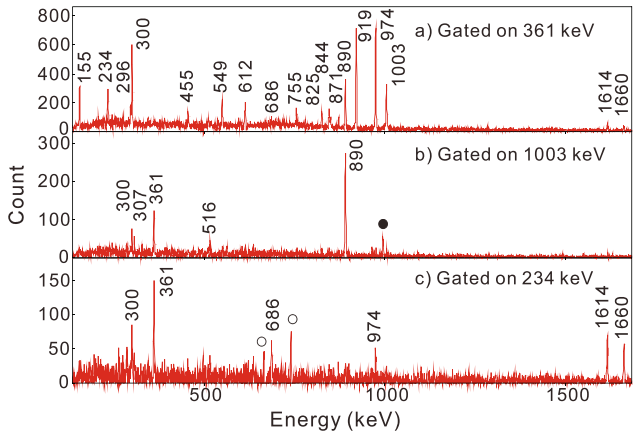

Fig. 3 (Color online) Typical coincidence spectra for ^{91}Ru gated on the 361, 1003, and 234 keV γ rays, corresponding to the transitions that depopulate the $15/2^-$ and $13/2^-$ states in ^{91}Ru. The 296, 300, 455, 549, 612, 755, 825, and 871 keV lines shown in the spectra belong to the transitions decaying the states of ^{91}Ru at the excitation energies above 2.5 MeV, thus these transitions did not present in the low-energy level scheme as shown in Fig. 1. Contaminant lines indicated with filled and open circles in the figure come from the $3p1n$ channel (^{90}Tc) and the $3p$ channel (^{91}Tc), respectively

γ rays fed into the ground state is observed. The ordering of the two new transitions is fixed by a newly observed 844 keV transition that crosses the transition sequence, as shown in Fig. 1. The normalized DCO ratio and asymmetry measured for the 890 keV transition are 0.63(5) and −0.03(1), respectively, indicating a stretched $M1$ multipolarity, which leads to the spin parity assignment of $11/2^+$ for the new state at 890 keV (denoted $11/2^+_1$ in the partial level scheme, as shown in Fig. 1). A stretched $E1$ character for the 1003 keV transition was obtained from the results of the normalized DCO ratio (0.59 ± 0.04) and linear polarization (0.12 ± 0.05) measurements. Thus, this γ-ray was assigned to the $13/2^- \rightarrow 11/2^+_1$ transition, which provides a supplementary argument for the previous assignment of the $13/2^-$ state at 1893 keV.

The newly observed γ-rays of 234 keV, 1660 keV, and 1614 keV were assigned to transitions between the $13/2^-$ level and the $9/2^+$ ground state. These new transitions are shown in Fig. 3. Based on the obtained normalized DCO ratios and Compton asymmetries, we assigned $M1$ and $E2$ multipolarities to 1660 keV and 1614 keV γ rays, respectively. The DCO ratio analysis shows that the 234 keV transition has dipole multipolarity (see Table 1). These assignments imply the existence of a $7/2^+$ state at 46 keV excitation energy and a second $11/2^+$ level at 1660 keV excitation energy (as shown in Fig. 1, marked $11/2^+_2$). The 46 keV γ-ray to the ground state cannot be observed in EXOGAM Clovers because it is fully absorbed by the material located around the target, including the DIAMANT array. In addition, a new transition of 686 keV was observed and assigned to connect the $11/2^+_2$ and $13/2^+$ states. The combination of the normalized DCO and linear polarization data shows that the 686 keV γ ray has $M1$ multipolarity, which confirms that the 1660 keV level has $J^\pi = 11/2^+$.

Table 1 γ-ray energies, intensities relative to the $13/2^+ \rightarrow 9/2^+$ 973.5 keV transition, DCO ratios, asymmetries, and initial and final spins for the transitions presented in the partial level scheme of ^{91}Ru as shown in Fig. 1. Energy uncertainties are within 0.5 keV. The gates used for determination of the DCO ratios are indicated in the table

E_γ (keV)	I_γ (%)	$R^{\text{exp}}_{\text{DCO}}$	Gate (keV)	a	$R^{\text{norm}}_{\text{DCO}}$	Asymmetry	$E_i \rightarrow J^\pi_f$
45.8 (5)							$7/2^+ \rightarrow 9/2^+$
155.4 (3)	3.0 (2)	0.65 (7)	974	1	0.65 (7)		$17/2^-_2 \rightarrow 15/2^-$
209.4 (2)	4.5 (2)						$17/2^-_2 \rightarrow 17/2^-_1$
233.6 (2)	2.7 (2)	0.9 (2)	361	0.6	0.54 (2)		$13/2^- \rightarrow 11/2^+_2$
306.8 (2)	1.9 (2)	1.04 (10)	974	1	1.04 (10)		$17/2^-_1 \rightarrow 13/2^-$
328.0 (2)	25.1 (1)	1.06 (5)	898	1	1.06 (5)	− 0.25 (4)	$17/2^-_1 \rightarrow 17/2^+_1$
360.6 (2)	5.9 (2)	0.68 (4)	974	1	0.68 (4)	− 0.15 (5)	$15/2^- \rightarrow 13/2^-$
497.2 (2)	38.3 (1)	1.07 (2)	974	1	1.07 (2)	0.17 (3)	$21/2^+ \rightarrow 17/2^+$
516.4 (3)	1.1 (1)	1.1 (1)	974	1	1.1 (1)	0.27 (5)	$17/2^-_2 \rightarrow 13/2^-$
685.8 (4)	0.8 (1)	0.6 (1)	974	1	0.6 (1)	− 0.12 (3)	$11/2^+_2 \rightarrow 13/2^+$
844.0 (4)	0.4 (1)						$11/2^+_1 \rightarrow 7/2^+$
889.8 (2)	7.6 (1)	1.05 (5)	361	0.6	0.63 (5)	− 0.03 (1)	$11/2^+_1 \rightarrow 9/2^+$
898.5 (1)	73 (1)	1.01 (1)	974	1	1.01 (1)	0.131 (6)	$17/2^+ \rightarrow 13/2^+$
919.8 (2)	11.3 (1)	0.99 (4)	974	1	0.99 (4)	− 0.07 (1)	$13/2^- \rightarrow 13/2^+$
973.5 (1)	100	0.98 (2)	497	1	0.98 (2)	0.139 (4)	$13/2^+ \rightarrow 9/2^+$
1003.6 (3)	6.7 (3)	0.98 (4)	361	0.6	0.59 (4)	0.12 (5)	$13/2^- \rightarrow 11/2^+_1$
1613.9 (3)	1.3 (1)	1.58 (9)	234	0.6	0.95 (9)	0.18 (3)	$11/2^+_2 \rightarrow 7/2^+$
1659.7 (4)	1.3 (1)	1.07 (8)	234	0.6	0.64 (8)	− 0.07 (2)	$11/2^+_2 \rightarrow 9/2^+$

4 Calculation and discussion

The low-energy level schemes of the $N = 47$ nuclei with $Z \geqslant 38$ display a complex structure in the presence of high-energy γ rays, irregular level spacings, and parallel decay branches, indicating the dominance of single-particle excitations or configurations associated with the weak coupling of a $g_{9/2}$ neutron hole to core excitations. The $7/2^+$, $11/2^+_1$, and $11/2^+_2$ states newly identified below the last $13/2^-$ level in ^{91}Ru were grouped into a positive-parity structure. Very similar structures have also been found previously in lighter $N = 47$ isotones, down to ^{85}Sr [3, 5–8], allowing a detailed study of level systematics with varying proton numbers.

Figure 4 compares the positive-parity structures and $13/2^-$ states in the $N = 47$ even-odd isotones from ^{85}Sr to ^{91}Ru. The 2^+_1 and 2^+_2 levels in the $N = 48$ even-even nuclei from ^{86}Sr to ^{92}Ru (except 2^+_2 in ^{92}Ru) are also shown [24–27]. Figure 4 shows that the energies of the two $11/2^+$ states and low-lying $7/2^+$ level in ^{91}Ru fit well with the level systematics of $N = 47$ isotones. Note that the systematic occurrence of low-lying $7/2^+$ states in the $N = 47$ nuclei is an important feature of the three-neutron-hole $\nu g_{9/2}^{-3}$ configuration [4, 28]. The energies of the $11/2^+_1$ levels in the $N = 47$ isotones from ^{85}Sr to ^{91}Ru agree well with those of the 2^+_1 states in the adjacent $N = 48$ even-even cores. The latter are known to be excitations dominated by a two-neutron–hole configuration $(\nu g_{9/2}^{-2})2^+$ [24, 27, 29, 30]. Based on energy systematics, it can be expected that the $11/2^+_1$ states arise from the coupling of a $g_{9/2}$ neutron hole to the 2^+ neutron core excitations, resulting in a three-neutron-hole configuration of $(\nu g_{9/2}^{-3})$ $11/2^+$. In particular, in the semi-magic nucleus ^{85}Sr with only three neutron holes outside the doubly closed-shell nucleus ^{88}Sr, the $7/2^+$ and $11/2^+_1$ states have been suggested as nearly pure $\nu g_{9/2}^{-3}$ excitations [1].

Figure 4 shows that the $11/2^+_2$ states remain almost constant as Z. This feature is also observed for the 2^+_2 levels in the $N = 48$ nuclei ^{86}Sr (1854 keV), ^{88}Zr (1818 keV), and ^{90}Mo (1897 keV), which lie at almost the same energy as the first-excited 2^+ state (1836 keV) in the ^{88}Sr core [31], varying by only 61 keV. The 2^+_1 level in ^{88}Sr is a proton core excited state, in which the main component is a proton 1p-1 h excitation from $\pi p_{3/2}$ into the $\pi p_{1/2}$ orbital [30, 31]. Therefore, it is reasonable to assume that the $11/2^+_2$ levels in the $N = 47$ isotones are associated with weak coupling of $\nu g_{9/2}$ neutron holes to the proton-core 2^+ excitation.

To confirm the validity of the above interpretation of the low-energy structure of $N = 47$ isotones, we performed a semiempirical shell model calculation, which is discussed in the next two subsections.

4.1 Semiempirical shell model calculations

The semiempirical shell model allows calculation of the excitation energy of the complex multi-particle-hole (p-h) configuration from the excitation energies of known configurations in neighboring nuclei. This method is parameter independent and was proposed by Garvey and Kelson [32, 33] for ground-state masses, based on prescriptions by Talmi and de-Shalit [34, 35].

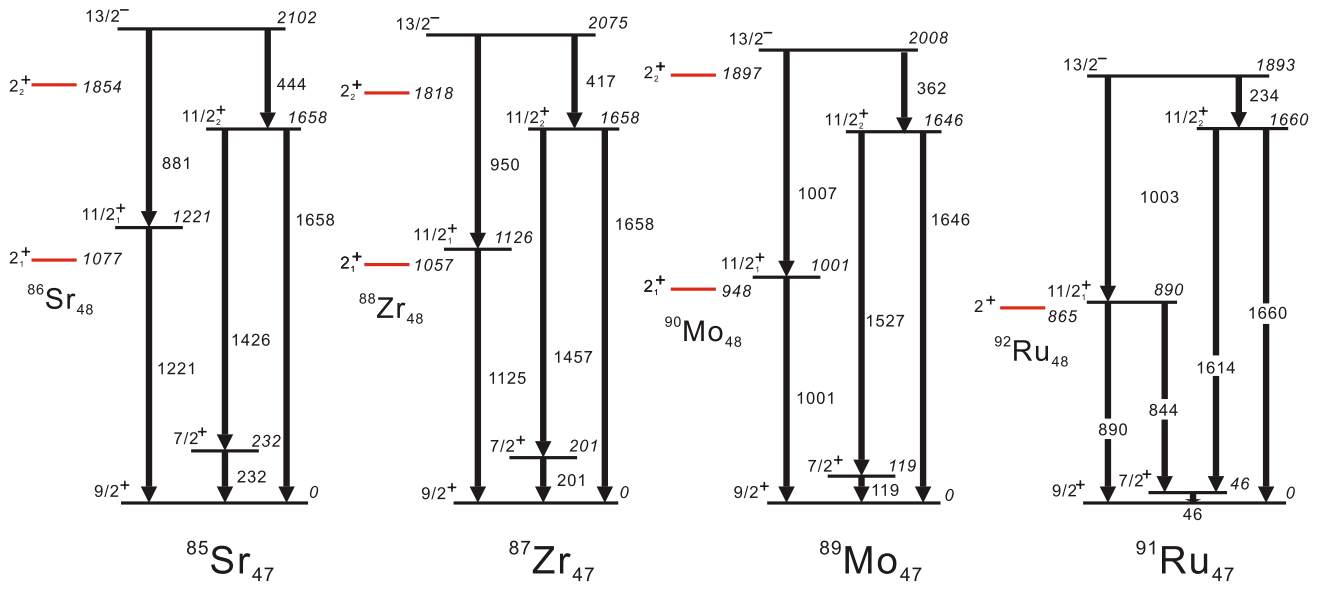

Fig. 4 (Color online) Level systematics of positive-parity structures below $13/2^-$ states in $N = 47$ even-odd isotones ^{85}Sr, ^{87}Zr, ^{89}Mo, and ^{91}Ru (present work). The 2^+_1 and 2^+_2 levels in the $N = 48$ even-even nuclei from ^{86}Sr to ^{92}Ru (except 2^+_1 in ^{92}Ru) are also shown (red)

This technique was later extended to calculate the excited states in the $A \sim 150$ and 200 mass regions by Blomqvist et al. [36], providing the framework that we use here. Usually, a specific level in a nucleus is not associated with a single configuration of quasiparticles but rather corresponds to a complex mixture of many configurations of the same spin and parity. However, in favorable cases, a level can have a simple structure, and its wave function is strongly dominated by a single configuration. In general, this requires the level to be well-separated from those of the same spin and parity, which can be fulfilled for particular yrast or near-yrast levels. In such cases, the multiparticle–hole configuration can be broken into simpler configurations with fewer particles by fractional parentage decomposition, where these simpler configurations correspond to specific levels in the neighboring nuclei. This implies a linear connection between the excitation energies of the levels and nuclear ground-state masses occurring in this reduction.

The nucleus ^{91}Ru has six proton particles and three neutron holes outside the ^{88}Sr core. For some of its states, specifically the $9/2^+$ ground state and the $7/2^+$ and $11/2^+_1$, it is assumed that the protons are in a seniority-zero ($\upsilon = 0$) configuration, and that the angular momentum is generated by the neutrons in the $g_{9/2}$ orbital. In this approximation, the states with spin J can be written as follows:

$$\left|{}^{91}\mathrm{Ru}_{47}(J)\right\rangle = \left|(\nu g_{9/2}^{-3})^{(J)}(\pi^6)^{(0)}_{\upsilon=0}\right\rangle, \tag{3}$$

where the configuration on the right-hand side corresponds to an ^{88}Sr core. This configuration can be decoupled as follows:

$$\left|(\nu g_{9/2}^{-3})^{(J)}(\pi^6)^{(0)}_{\upsilon=0}\right\rangle_{^{91}\mathrm{Ru}} = \left|(\nu g_{9/2}^{-3})^{(J)}\right\rangle_{^{85}\mathrm{Sr}} \otimes \left|(\pi^6)^{(0)}_{\upsilon=0}\right\rangle_{^{94}\mathrm{Ru}}. \tag{4}$$

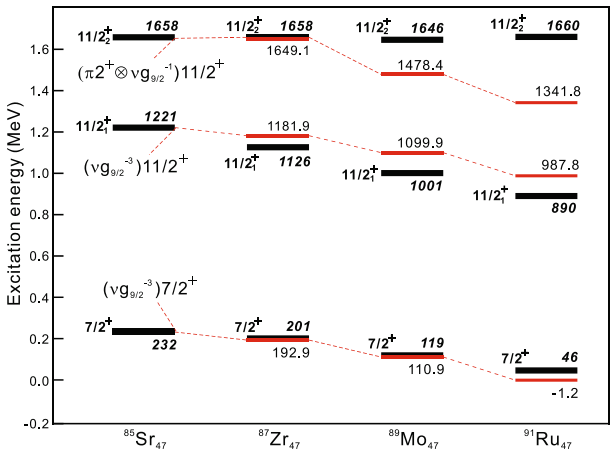

Fig. 5 (Color online) Calculated level energies, using the semiempirical shell model, of the $7/2^+$, $11/2^+_1$, and $11/2^+_2$ states in the even-odd $N = 47$ isotones ^{87}Zr, ^{89}Mo, and ^{91}Ru (red lines) are compared to the experimental data (black bars)

The semiempirical shell model then yields the following expression for the energies of these states in ^{91}Ru:

$$\begin{aligned} E^{^{91}\mathrm{Ru}}_{(\pi^6_{0^+}\nu g^{-3}_{9/2})J} = {} & E^{^{85}\mathrm{Sr}}_{(\nu g^{-3}_{9/2})J} + 2E^{^{93}\mathrm{Ru}}_{(\pi^6_{0^+}\nu g^{-1}_{9/2})9/2^+} + E^{^{86}\mathrm{Sr}}_{(\nu g^{-2}_{9/2})0^+} \\ & - E^{^{94}\mathrm{Ru}}_{(\pi^6_{0^+})0^+} - 2E^{^{87}\mathrm{Sr}}_{(\nu g^{-1}_{9/2})9/2^+} - E^{^{85}\mathrm{Sr}}_{(\nu g^{-3}_{9/2})9/2^+} \\ & - E^{^{92}\mathrm{Ru}}_{(\pi^6_{0^+})0^+\nu g^{-2}_{9/2})0^+} + S \end{aligned} \tag{5}$$

This relation between the energies of the states in ^{91}Ru is obtained by counting the interactions. The first line in Eq. (5) lists the contributions of the neutron-neutron and neutron-proton interactions. The second line corrects for over-counting in the first line of the proton-proton interaction and the neutron single-particle energy, while its last term accounts for the ground-state masses of the related nuclei:

$$\begin{aligned} S = {} & 2M_{^{93}\mathrm{Ru}} + M_{^{88}\mathrm{Sr}} + M_{^{86}\mathrm{Sr}} \\ & - 2M_{^{87}\mathrm{Sr}} - M_{^{94}\mathrm{Ru}} - M_{^{92}\mathrm{Ru}} = -233.2\ \mathrm{keV}. \end{aligned} \tag{6}$$

For example, with the known excitation energies of the concerned configurations in neighboring nuclei, the energy of the $(\pi^6_{0^+}\nu g^{-3}_{9/2})11/2^+$ state ^{91}Ru is calculated as:

$$\begin{aligned} E^{^{91}\mathrm{Ru}}_{(\pi^6_{0^+}\nu g^{-3}_{9/2})11/2^+} = {} & E^{^{85}\mathrm{Sr}}_{(\nu g^{-3}_{9/2})11/2^+} + 2E^{^{93}\mathrm{Ru}}_{(\pi^6_{0^+}\nu g^{-1}_{9/2})9/2^+} \\ & + E^{^{86}\mathrm{Sr}}_{(\nu g^{-2}_{9/2})0^+} - E^{^{94}\mathrm{Ru}}_{(\pi^6_{0^+})0^+} - 2E^{^{87}\mathrm{Sr}}_{(\nu g^{-1}_{9/2})9/2^+} \\ & - E^{^{85}\mathrm{Sr}}_{(\nu g^{-3}_{9/2})9/2^+} - E^{^{92}\mathrm{Ru}}_{(\pi^6_{0^+})0^+(\nu g^{-2}_{9/2})0^+} + S \\ = {} & 1221\ \mathrm{keV} + 2\times 0\ \mathrm{keV} + 0\ \mathrm{keV} - 0\ \mathrm{keV} \\ & - 2\times 0\ \mathrm{keV} - 0\ \mathrm{keV} - 0\ \mathrm{keV} + S \\ = {} & 987.8\ \mathrm{keV}. \end{aligned} \tag{7}$$

4.2 Results

The calculated results for the $7/2^+$, $11/2^+_1$, and $11/2^+_2$ states of the $N = 47$ isotones are shown in Fig. 5 (red lines). Input data for the calculation are taken from the neighboring nuclei $^{85-87}$Sr [1, 24, 37], $^{88-90}$Zr [4, 25, 38, 39], $^{90-92}$Mo [26, 40, 41], and $^{92-94}$Ru [27, 42, 43]. The ground-state masses required for the calculations were obtained from Ref. [44]). The calculation details are as follows:

The energy of the $7/2^+$ state of ^{91}Ru from the $(\pi^6_{0^+}\nu g^{-3}_{9/2})7/2^+$ configuration was calculated as

$$
\begin{aligned}
E^{^{91}\mathrm{Ru}}_{(\pi^6_{0^+}\nu g^{-3}_{9/2})7/2^+} &= E^{^{85}\mathrm{Sr}}_{(\nu g^{-3}_{9/2})7/2^+} + 2E^{^{93}\mathrm{Ru}}_{(\pi^6_{0^+}\nu g^{-1}_{9/2})9/2^+} + E^{^{86}\mathrm{Sr}}_{(\nu g^{-2}_{9/2})0^+} \\
&\quad - E^{^{94}\mathrm{Ru}}_{(\pi^6_{0^+})0^+} - 2E^{^{87}\mathrm{Sr}}_{(\nu g^{-1}_{9/2})9/2^+} \\
&\quad - E^{^{85}\mathrm{Sr}}_{(\nu g^{-3}_{9/2})9/2^+} - E^{^{92}\mathrm{Ru}}_{(\pi^6_{0^+})0^+(\nu g^{-2}_{9/2})0^+} + S \\
&= 232\ \mathrm{keV} + 2\times 0\ \mathrm{keV} + 0\ \mathrm{keV} - 0\ \mathrm{keV} \\
&\quad - 2\times 0\ \mathrm{keV} - 0\ \mathrm{keV} - 0\ \mathrm{keV} - 233.2\ \mathrm{keV} \\
&= -1.2\ \mathrm{keV}.
\end{aligned} \tag{8}
$$

with two protons less than ^{91}Ru, the nucleus ^{89}Mo will have seven quasiparticles relative to the ^{88}Sr core. The energy of the $(\pi^4_{0^+}\nu g^{-3}_{9/2})11/2^+$ state was calculated as

$$
\begin{aligned}
E^{^{89}\mathrm{Mo}}_{(\pi^4_{0^+}\nu g^{-3}_{9/2})11/2^+} &= E^{^{85}\mathrm{Sr}}_{(\nu g^{-3}_{9/2})11/2^+} + 2E^{^{91}\mathrm{Mo}}_{(\pi^4_{0^+}\nu g^{-1}_{9/2})9/2^+} \\
&\quad + E^{^{86}\mathrm{Sr}}_{(\nu g^{-2}_{9/2})0^+} - E^{^{92}\mathrm{Mo}}_{(\pi^4_{0^+})0^+} - 2E^{^{87}\mathrm{Sr}}_{(\nu g^{-1}_{9/2})9/2^+} \\
&\quad - E^{^{85}\mathrm{Sr}}_{(\nu g^{-3}_{9/2})9/2^+} - E^{^{90}\mathrm{Mo}}_{(\pi^4_{0^+})0^+(\nu g^{-2}_{9/2})0^+} + S \\
&= 1221\ \mathrm{keV} + 2\times 0\ \mathrm{keV} + 0\ \mathrm{keV} - 0\ \mathrm{keV} \\
&\quad - 2\times 0\ \mathrm{keV} - 0\ \mathrm{keV} - 0\ \mathrm{keV} + S \\
&= 1099.9\ \mathrm{keV},
\end{aligned} \tag{9}
$$

In this reduction, the mass term S is

$$
\begin{aligned}
S &= 2M_{^{91}\mathrm{Mo}} + M_{^{88}\mathrm{Sr}} + M_{^{86}\mathrm{Sr}} - 2M_{^{87}\mathrm{Sr}} \\
&\quad - M_{^{92}\mathrm{Mo}} - M_{^{90}\mathrm{Mo}} = -121.1\ \mathrm{keV}.
\end{aligned} \tag{10}
$$

Using a similar calculation, the excitation energy of the $(\pi^4_{0^+}\nu g^{-3}_{9/2})7/2^+$ state was deduced as 110.9 keV. Based on these considerations, the excitation energies of the five quasiparticle seniority-three $(\pi^2_{0^+}\nu g^{-3}_{9/2})$, $11/2^+$ and $7/2^+$ configurations in ^{87}Zr were calculated as 1181.9 keV and 192.9 keV.

As argued above, the $11/2^+_2$ state in the $N = 47$ isotones arises from the weak coupling of nucleons to the 2^+_1 level of ^{88}Sr, which is interpreted as a proton p-h core excitation. In ^{85}Sr, the three-quasiparticle weak-coupling state of $[(\pi p^{-1}_{3/2}\pi p_{1/2})^{2^+}(\nu g^{-3}_{9/2})^{9/2^+}_{\upsilon=1}]11/2^+$ was observed at 1658 keV, where it is suggested that the three neutron holes are in a seniority $\upsilon = 1$ configuration. The appropriate configuration for this state in ^{91}Ru is $[(\pi^6)^{0^+}_{\upsilon=0}(\pi p^{-1}_{3/2}\pi p_{1/2})^{2^+}(\nu g^{-3}_{9/2})^{9/2^+}_{\upsilon=1}]11/2^+$ in which the p-h excitation is coupled to a six-proton-particle configuration with seniority $\upsilon = 0$. The calculation of the excitation energy of this nine-quasiparticle state can start from the corresponding quantity in ^{85}Sr and yields

$$
\begin{aligned}
&E^{^{91}\mathrm{Ru}}_{[(\pi^6)^{0^+}_{\upsilon=0}(\pi p^{-1}_{3/2}\pi p_{1/2})^{2^+}(\nu g^{-3}_{9/2})^{9/2^+}_{\upsilon=1}]11/2^+} \\
&\quad = E^{^{85}\mathrm{Sr}}_{[(\pi p^{-1}_{3/2}\pi p_{1/2})^{2^+}(\nu g^{-3}_{9/2})^{9/2^+}_{\upsilon=1}]11/2^+} + E^{^{92}\mathrm{Ru}}_{(\pi^6)^{0^+}_{\upsilon=0}(\nu g^{-2}_{9/2})^{0^+}_{\upsilon=0}} \\
&\qquad + E^{^{93}\mathrm{Ru}}_{(\pi^6)^{0^+}_{\upsilon=0}(\nu g^{-1}_{9/2})} - E^{^{94}\mathrm{Ru}}_{(\pi^6)^{0^+}_{\upsilon=0}} - E^{^{86}\mathrm{Sr}}_{(\nu g^{-2}_{9/2})^{0^+}_{\upsilon=0}} - E^{^{87}\mathrm{Sr}}_{\nu g^{-1}_{9/2}} + S \\
&= 1658\ \mathrm{keV} + 0\ \mathrm{keV} + 0\ \mathrm{keV} - 0\ \mathrm{keV} \\
&\quad - 0\ \mathrm{keV} - 0\ \mathrm{keV} + S \\
&\quad = 1341.8\ \mathrm{keV}.
\end{aligned} \tag{11}
$$

In this case, the mass term S is

$$
\begin{aligned}
S &= M_{^{85}\mathrm{Sr}} + M_{^{92}\mathrm{Ru}} + M_{^{93}\mathrm{Ru}} + M_{^{88}\mathrm{Sr}} - M_{^{94}\mathrm{Ru}} \\
&\quad - M_{^{86}\mathrm{Sr}} - M_{^{87}\mathrm{Sr}} - M_{^{91}\mathrm{Ru}} = -316.2\ \mathrm{keV}.
\end{aligned} \tag{12}
$$

The excitation energy of the seven-quasiparticle $[(\pi^4)^{0+}_{\upsilon=0}(\pi p^{-1}_{3/2}\pi p_{1/2})^{2+}(\nu g^{-3}_{9/2})^{9/2+}_{\upsilon=1}]11/2^+$ state in ^{89}Mo is calculated in a similar approach as above to be

$$
\begin{aligned}
&E^{^{89}\mathrm{Mo}}_{[(\pi^4)^{0^+}_{\upsilon=0}(\pi p^{-1}_{3/2}\pi p_{1/2})^{2^+}(\nu g^{-3}_{9/2})^{9/2^+}_{\upsilon=1}]11/2^+} \\
&\quad = E^{^{85}\mathrm{Sr}}_{[(\pi p^{-1}_{3/2}\pi p_{1/2})^{2^+}(\nu g^{-3}_{9/2})^{9/2^+}_{\upsilon=1}]11/2^+} + E^{^{90}\mathrm{Mo}}_{(\pi^4)^{0^+}_{\upsilon=0}(\nu g^{-2}_{9/2})^{0^+}_{\upsilon=0}} \\
&\qquad + E^{^{91}\mathrm{Mo}}_{(\pi^4)^{0^+}_{\upsilon=0}(\nu g^{-1}_{9/2})} - E^{^{92}\mathrm{Mo}}_{(\pi^4)^{0^+}_{\upsilon=0}} - E^{^{86}\mathrm{Sr}}_{(\nu g^{-2}_{9/2})^{0^+}_{\upsilon=0}} - E^{^{87}\mathrm{Sr}}_{\nu g^{-1}_{9/2}} + S \\
&\quad = 1658\ \mathrm{keV} + 0\ \mathrm{keV} + 0\ \mathrm{keV} - 0\ \mathrm{keV} - 0\ \mathrm{keV} - 0\ \mathrm{keV} + S \\
&\quad = 1478.4\ \mathrm{keV}.
\end{aligned} \tag{13}
$$

The mass term S is

$$
\begin{aligned}
S &= M_{^{85}\mathrm{Sr}} + M_{^{90}\mathrm{Mo}} + M_{^{91}\mathrm{Mo}} + M_{^{88}\mathrm{Sr}} - M_{^{92}\mathrm{Mo}} \\
&\quad - M_{^{86}\mathrm{Sr}} - M_{^{87}\mathrm{Sr}} - M_{^{89}\mathrm{Mo}} = -179.6\ \mathrm{keV}.
\end{aligned} \tag{14}
$$

A similar calculation gives a value of 1649.1 keV for the excitation energy of the five-quasiparticle configuration $[(\pi^2)^{0^+}_{\upsilon=0}(\pi p^{-1}_{3/2}\pi p_{1/2})^{2^+}(\nu g^{-3}_{9/2})^{9/2^+}_{\upsilon=1}]11/2^+$ in ^{87}Zr.

A comparison between the semiempirical shell model calculation and the experimental observations is shown in Fig. 5. The figure shows that the estimate based on the three-neutron-hole $\nu g^{-3}_{9/2}$ structure provides an excellent description of the decreasing excitation energies of the $7/2^+$ and $11/2^+_1$ levels along the $N = 47$ isotonic chain. This trend reflects the behavior of the seniority scheme, in which the $\nu g^{-3}_{9/2}$ configuration gradually falls in energy as the $g_{9/2}$ proton shell is filled until midshell. It can be seen in Fig. 5 that the difference between the experimental energy and the theoretical value for the $7/2^+$ level is only 8 keV for both ^{87}Zr and ^{89}Mo, and 47 keV for ^{91}Ru. However, the deviation becomes higher in the case of $11/2^+_1$. The value was 56 keV in ^{87}Zr and then increased to almost 100 keV in both ^{89}Mo and ^{91}Ru. This indicates that the low-lying $7/2^+$ levels of the $N = 47$ isotones originate from the configuration $\nu g^{-3}_{9/2}$ and remain quite pure with increasing Z until ^{91}Ru. However, the $11/2^+_1$ state would have smoothly increasing configuration mixing

from ^{87}Zr to ^{91}Ru, whereas this state might also be dominated by the $\nu g_{9/2}^{-3}$ configuration. It is shown in Fig. 5 that the calculated weak-coupling state of $(\pi 2^+ \nu g_{9/2}^{-1})11/2^+$ reproduces the experimentally observed $11/2_2^+$ level for ^{87}Zr with a deviation of only 9 keV. Note, however, that the deviation amounts to 168 keV and 318 keV as the calculation goes to the heavier isotones ^{89}Mo and ^{91}Ru, respectively. These larger deviations were possibly due to significant mixing from the other configurations.

Note that the $11/2_1^+$ and $11/2_2^+$ states were observed in the same low-spin-level schemes, lying close in energy. Owing to the energy proximity and spin-parity identity, it is most likely that the two $11/2^+$ states are admixed with each other. This might account for the above finding that, compared to the $7/2^+$ case, the $11/2_1^+$ and $11/2_2^+$-level energies deviate more strongly from the experiment for both ^{89}Mo and ^{91}Ru, with the mixing likely being more significant in magnitude. Under the assumption of two-state mixing between $(\nu g_{9/2}^{-3})11/2^+$ and $(\pi 2^+ \nu g_{9/2}^{-1})11/2^+$, we have estimated the percentages of the $\nu g_{9/2}^{-3}$ components of the $11/2_1^+$ states in each even-odd $N = 47$ isotone by using the semiquantitative two-state mixing calculation (cf. Ref. [45]). The calculated results show that the $\nu g_{9/2}^{-3}$ configuration contributes 94%, 79%, and 73% of the wave functions to the $11/2_1^+$ states of ^{87}Zr, ^{89}Mo, and ^{91}Ru, respectively. These data clearly demonstrate that the two $11/2^+$ states in the $N = 47$ isotones are correlated, and that the mixing between the two states gradually increases with increasing proton number. This is a general property of the np interaction that strongly breaks seniority and further enhances the correlation as each proton is added to the ^{88}Sr core, resulting in a strong seniority violation in ^{91}Ru.

The final remark concerns the $11/2_2^+$ state. Its energy remains almost constant with increasing proton number, which is quite different from the behaviors of the $7/2^+$ and $11/2_1^+$ levels, where the energy level is systematically lower. The main reason behind this $11/2_2^+$ evolution is the basic feature of a quantum system arising from the mixing of two states: the unperturbed states repel each other, thereby increasing the energy of the upper state, which further increases the energy of the upper state and cancels the energy dropping effect of the unperturbed $11/2_2^+$ state with increasing Z, resulting in the observed constancy of its energy.

5 Summary

The excited states in ^{91}Ru were populated via the fusion-evaporation reaction ^{58}Ni(^{36}Ar, $2p1n\gamma$)^{91}Ru at a beam energy of 111 MeV. Spins and parities were assigned by measuring the DCO ratios and the linear polarization of γ rays. Three low-energy states with spins $7/2^+$, $11/2_1^+$, and $11/2_2^+$ were identified in ^{91}Ru for the first time and fitted the level systematics of $N = 47$ even-odd isotones. A semiempirical shell model was used to explain the systematics of these positive-parity states in the $N = 47$ isotones. The calculations reproduced the energy spectra of $N = 47$ isotones up to ^{91}Ru. Based on a semiquantitative calculation of two-state mixing, it was found that seniority is increasingly broken in the first excited $11/2^+$ state as protons are added to the ^{88}Sr core, resulting in a gradually stronger violation from ^{87}Zr to ^{91}Ru.

Acknowledgements The authors thank the operators of the GANIL cyclotrons for providing the ^{36}Ar beam. We would also like to thank the EXOGAM collaboration for the use of the clover Ge detector array and the DIAMANT collaboration for the use of the charged particle detector system and the European γ-ray Spectroscopy Pool for use in neutron detector systems.

Author contributions All authors contributed to the study conception and design. Material preparation, data collection and analysis were performed by Yong Zheng, Meng Wang, Min-Liang Liu and Kai-Long Wang. The first draft of the manuscript was written by Yong Zheng and all authors commented on the previous versions of the manuscript. All authors read and approved the final manuscript.

Data availability The data that support the findings of this study are openly available in Science Data Bank at https://cstr.cn/31253.11.sciencedb.25337 and https://doi.org/10.57760/sciencedb.25337.

Declarations

Conflict of interest The authors declare that they have no conflict of interest.

References

1. S.E. Arnell, S. Sjöberg, Ö. Skeppstedt, E. Wallander, High-spin states of ^{85}Sr. Nucl. Phys. A **280**, 72 (1977). https://doi.org/10.1016/0375-9474(77)90294-9
2. L. Lühmann, K.P. Lieb, A. Moussavi-Zarandi et al., Yrast transition strengths in ^{85}Rb and ^{85}Sr. Z. Phys. A **313**, 297 (1983). https://doi.org/10.1007/BF01439482
3. S. Kumar, N. Kumar, S. Mandal et al., High spin band structure of $^{85}_{38}Sr_{47}$. Phys. Rev. C **90**, 024315 (2014). https://doi.org/10.1103/PhysRevC.89.034303
4. J.E. Kitching, P.A. Batay-Csorba, C.A. Fields et al., High spin states in ^{88,87,86}Zr. Nucl. Phys. A **302**, 159 (1978). https://doi.org/10.1016/0375-9474(78)90292-0
5. P. Banerjee, S. Ganguly, M.K. Pradhan et al., Spectroscopy of weakly deformed bands in ^{87}Zr: First observation of the shears mechanism in a Zr isotope. Phys. Rev. C **98**, 034320 (2018). https://doi.org/10.1103/PhysRevC.98.034320
6. M. Weiszflog, D. Rudolph, C.J. Gross et al., Identification and structure of high spin particle-hole states in ^{89}Mo. Z. Phys. A **344**, 395 (1993). https://doi.org/10.1007/BF01283194
7. G. Garcia-Bermudez, M.A. Cardona, R.V. Ribas et al., Level structure of ^{89}Mo. Phys. Rev. C **48**, 1623 (1993). https://doi.org/10.1103/PhysRevC.48.1623
8. D. Zainea, D. Rudolph, A. Harder et al., Electromagnetic decay strengths in the isobars ^{89}Nb, ^{89}Mo and ^{89}Tc. Z. Phys. A **352**, 365 (1995). https://doi.org/10.1007/BF01299754

9. S.E. Arnell, D. Foltescu, H.A. Roth et al., First information about the level structure of ^{91}Ru. Phys. Scr. **47**, 355 (1993). https://doi.org/10.1088/0031-8949/47/3/005
10. J. Heese, H. Grawe, K.H. Maier et al., High spin states and shell model description of the neutron deficient nuclei ^{90}Ru and ^{91}Ru. Phys. Rev. C **49**, 1896 (1994). https://doi.org/10.1103/PhysRevC.49.1896
11. S.H. Zhu, T.L. Zhao, X.J. Bao, Systematic study of the synthesis of heavy and superheavy nuclei in ^{48}Ca-induced fusion-evaporation reactions. Nucl. Sci. Tech. **35**, 124 (2024). https://doi.org/10.1007/s41365-024-01483-5
12. P.H. Chen, H. Wu, Z.X. Yang et al., Prediction of synthesis cross sections of new Moscovium isotopes in fusion-evaporation reactions. Nucl. Sci. Tech. **34**, 7 (2023). https://doi.org/10.1007/s41365-022-01157-0
13. Z. Wang, Z.Z. Ren, Predictions of the decay properties of the superheavy nuclei ^{293,294}119 and ^{294,295}120. Nucl. Tech. **46**, 080011 (2023). https://doi.org/10.11889/j.0253-3219-2023.hjs.46.080011. (**in Chinese**)
14. X.C. Han, S. Wang, H.Y. Wu et al., CsI-Bowl: an ancillary detector for exit channel selection in γ-ray spectroscopy experiments. Nucl. Sci. Tech. **34**, 133 (2023). https://doi.org/10.1007/s41365-023-01289-x
15. J.N. Scheurer, M. Aiche, M.M. Aleonard et al., Improvements in the in-beam γ-ray spectroscopy provided by an ancillary detector coupled to a Ge γ-spectrometer: the DIAMANT-EUROGAM II example. Nucl. Instrum. Methods Phys. Res. A **385**, 501 (1997). https://doi.org/10.1016/S0168-9002(96)01038-8
16. J. Gál, G. Hegyesi, J. Molnár et al., The VXI electronics of the DIAMANT particle detector array. Nucl. Instrum. Methods Phys. Res. A **516**, 502 (2004). https://doi.org/10.1016/j.nima.2003.08.158
17. Ö. Skeppstedt, H.A. Roth, L. Lindström et al., The EUROBALL neutron wall design and performance tests of neutron detectors. Nucl. Instrum. Methods Phys. Res. A **421**, 531 (1999). https://doi.org/10.1016/S0168-9002(98)01208-X
18. J. Simpson, F. Azaiez, G. de France et al., The EXOGAM array: a radioactive beam gamma-ray spectrometer. Acta Phys. Hung. New Ser. Heavy Ion Phys. **11**, 159 (2000). https://www.researchgate.net/publication/233639747
19. B. Cederwall, F. Ghazi Moradi, T. Bäck et al., Evidence for a spin-aligned neutron-proton paired phase from the level structure of ^{92}Pd. Nature **469**, 68 (2011). https://doi.org/10.1038/nature09644Letter
20. K.S. Krane, R.M. Steffen, R.M. Wheeler, Directional correlations of gamma radiations emitted from nuclear states oriented by nuclear reactions or cryogenic methods. Nucl. Data Tables **11**, 351 (1973). https://doi.org/10.1016/S0092-640X(73)80016-6
21. B. Schlitt, U. Maier, H. Friedrichs et al., A sectored Ge-Compton polarimeter for parity assignments in photon scattering experiments. Nucl. Instrum. Methods Phys. Res. A **337**, 416 (1994). https://doi.org/10.1016/0168-9002(94)91111-8
22. M. Piiparinen, A. Ataç, J. Blomqvist et al., High-spin spectroscopy of the ^{142}Eu, ^{143}Eu and ^{144}Eu nuclei. Nucl. Phys. A **605**, 191 (1996). https://doi.org/10.1016/0375-9474(96)00157-1
23. D. Sohler, I. Kuti, J. Timár et al., High-spin structure of ^{104}Pd. Phys. Rev. C **85**, 044303 (2012). https://doi.org/10.1103/PhysRevC.85.044303
24. C.A. Fields, F.W.N. de Boer, J. Sau, A study of the ^{84}Kr(α, 2nγ)^{86}Sr reaction. Nucl. Phys. A **398**, 512 (1983). https://doi.org/10.1016/0375-9474(83)90299-3
25. K. Oxorn, S.K. Mark, J.E. Kitching et al., High-spin states in ^{89}Nb, ^{88}Zr and ^{88}Nb with a shell-model description of the $N = 48$ and $N = 47$ nuclei. Z. Phys. A **321**, 485 (1985). https://doi.org/10.1007/BF01411984
26. M.K. Kabadiyski, F. Cristancho, C.J. Gross et al., A study of high spin states in the transitional nucleus ^{90}Mo. Z. Phys. A **343**, 165 (1992). https://doi.org/10.1007/BF01291821
27. S.E. Arnell, D. Foltescu, H.A. Roth et al., The level structure of ^{92}Ru up to high spin values. Z. Phys. A **346**, 111 (1993). https://doi.org/10.1007/BF01294626
28. I. Talmi, I. Unna, Energy levels and configuration interaction in Zr^{90} and related nuclei. Nucl. Phys. **19**, 225 (1960). https://doi.org/10.1016/0029-5582(60)90234-0
29. T.J. Mertzimekis, A.E. Stuchbery, N. Benczer-Koller et al., Systematics of first 2^+ state g factors around mass 80. Phys. Rev. C **68**, 054304 (2003). https://doi.org/10.1103/PhysRevC.68.054304
30. H. Duckwitz, P. Petkov, T. Thomas et al., Nuclear structure investigations of ^{84}Sr and ^{86}Sr using γ-ray spectroscopic methods. Nucl. Phys. A **965**, 13 (2017). https://doi.org/10.1016/j.nuclphysa.2017.05.077
31. E.A. Stefanova, R. Schwengner, J. Reif et al., Influence of neutron-core excitations on high-spin states in ^{88}Sr. Phys. Rev. C **62**, 054314 (2000). https://doi.org/10.1103/PhysRevC.62.054314
32. G.T. Garvey, T. Kelson, New nuclidic mass relationship. Phys. Rev. Lett. **16**, 197 (1966). https://doi.org/10.1103/PhysRevLett.16.197
33. G.T. Garvey, Nuclear mass relations. Annu. Rev. Nucl. Sci. **19**, 433 (1969). https://doi.org/10.1146/annurev.ns.19.120169.002245
34. I. Talmi, Effective interactions and coupling schemes in nuclei. Rev. Mod. Phys. **34**, 704 (1962). https://doi.org/10.1103/RevModPhys.34.704
35. A. de Shalit, I. Talmi, *Nuclear shell theory* (Academic, New York, 1963)
36. J. Blomqvist, P. Kleinheinz, P.J. Daly, Atomic masses above ^{146}Gd derived from a shell model analysis of high spin states. Z. Phys. A **312**, 27 (1983). https://doi.org/10.1007/BF01411658
37. L.P. Ekström, G.D. Jones, F. Kearns et al., Gamma-ray spectroscopy on ^{87}Sr and the energy-B(E2) rule. J. Phys. G Nucl. Phys. **7**, 85 (1981). https://doi.org/10.1088/0305-4616/7/1/013
38. S. Saha, R. Palit, J. Sethi et al., Experimental investigation of shell-model excitations of ^{89}Zr up to high spin. Phys. Rev. C **86**, 034315 (2012). https://doi.org/10.1103/PhysRevC.86.034315
39. E.K. Warburton, J.W. Olness, C.J. Lister et al., High-spin state spectroscopy of ^{88,90}Zr. Phys. Rev. C **31**, 1184 (1985). https://doi.org/10.1103/PhysRevC.31.1184
40. S. Ray, N.S. Pattabiraman, R. Goswami et al., Experimental study of nuclear structure of ^{91}Mo at high spin. Phys. Rev. C **69**, 054314 (2004). https://doi.org/10.1103/PhysRevC.69.054314
41. P. Singh, R.G. Pillay, J.A. Sheikh et al., Spectroscopy of high spin states in ^{92}Mo and ^{90}Mo. Phys. Rev. C **45**, 2161 (1992). https://doi.org/10.1103/PhysRevC.45.2161
42. P. Komninos, E. Nolte, P. Blasi, The 2.6 µs $(21/2)^+$ Isomer in ^{93}Ru. Z. Phys. A **310**, 137 (1983). https://doi.org/10.1007/BF01433624
43. W.J. Mills, J.J. Ressler, R.A.E. Austin et al., Search for the low-lying $(\pi 1g_{9/2})^4 6_2^+$ state in ^{94}Ru. Phys. Rev. C **75**, 047302 (2007). https://doi.org/10.1103/PhysRevC.75.047302
44. The 2020 Update to the Atomic Mass Evaluation. https://amdc.impcas.ac.cn/web/masseval.html
45. R. Casten, *Nuclear Structure from a Simple Perspective* (Oxford University Press, Cary, NC, 1990)